Anomalous, hysteretic, transverse magnetoresistance in superconducting thin films with magnetic vortex arrays

J. E. Villegas,[1,2,a)] A. Sharoni,[2] C.-P. Li,[2] and Ivan K. Schuller[2,b)]

[1]*Unité Mixte de Physique CNRS/Thales, Campus de Polytechnique,1 Avenue A. Fresnel, 91767 Palaiseau, France and Université Paris Sud 11, 91405 Orsay, France*
[2]*Department of Physics, University of California–San Diego, 9500 Gilman Drive, La Jolla, California 92093-0319, USA*

We have studied a superconducting/ferromagnetic hybrid system in which the normal to superconducting phase transition is controlled by the magnetic history. An anomalous transverse resistance appears at the phase transition, which shows magnetic hysteresis and a strong current dependence. We show that the anomaly originates from current redistributions due to the inhomogeneous superconductivity of this system. © *2009 American Institute of Physics.*
[DOI: 10.1063/1.3159466]

Nanoscale superconducting/ferromagnetic (S/F) hybrids often exhibit uncommon physical properties, due to the mutual interaction between the competing S and F orders.[1,2] In addition to their fundamental interest, they can be exploited for modern concept devices.[3] We study here a S/F hybrid in which the F magnetic hysteresis is imprinted into the properties of the S subsystem: due to the effect of the stray magnetic fields from the F subsystem, the hybrid's remanent state is either S or normal (N) depending on the magnetic history. Interestingly, this bistability makes of this system a simple S memory. We found that, as the hybrid is driven from the S into the N state (or vice versa), a very unusual anomalous voltage develops *perpendicular* to the injected electrical current. The transverse resistance associated with this voltage shows a strong magnetic hysteresis and a very singular current dependence. These properties do not correspond to those of the conventional Hall effect: they appear with the magnetic field applied *in plane* and are *not odd* with respect to the applied field nor the magnetization. We developed a model which shows that the anomalous transverse resistance is caused by current redistribution effects due to inhomogeneous superconductivity. These results rule out flux dynamics[4] and charge imbalance[5,6] related mechanisms, which are usually evoked to explain "even Hall effects" and resistance anomalies in superconductors.

The hybrid consists of a dense array of Fe nanodots (20 nm thick) prepared using nanoporous alumina masks[7] and covered with a superconducting Al thin film. A series of samples with different Al thickness t_{Al}, dot diameters $\varnothing$, and interdot distances d were prepared (see Table I). A 1 nm thick Au capping layer was deposited *in situ* on the Fe nanodots prior to Al evaporation (except for sample V13). The arrays show short-range hexagonal order [inset in Fig. 1(a)] and narrow Gaussian $\varnothing$ and d distributions ($\Delta\varnothing \leq \pm 15\%$, $\Delta d \leq \pm 20\%$). Coherence and penetration lengths, in the range of $\xi(0) \approx 45–50$ nm and $\lambda(0) \approx 250–400$ nm, respectively,[8] imply that the Al films are type-II superconductors. Further characterization can be found elsewhere.[7–9] Samples were optically lithographed with a cross-shaped bridge 40

$\times 40$ μm^2 [insets in Figs. 1(b) and 1(c)], which allows the measurement of voltages parallel (V_{XX}) and perpendicular (V_{XY}) to the injected electrical current J. The magnetization and magnetoresistance data shown in Figs. 1 and 2 correspond to sample P5. Qualitatively, the same behavior is observed for all the studied samples.

Figure 1(a) shows magnetization versus in-plane applied field $M(H)$ at $T=6$ K. Note in the major loop (circles) the "pinching" around the coercive fields and the almost linear virgin curves (black lines) that quickly merge the major loop. These characteristics are the "fingerprints"[9] of the nucleation, displacement, and annihilation of magnetic vortices in the nanodots during magnetic reversal[8–10] [see a cartoon of this mechanism in Fig. 1(a)]. In a magnetic vortex the magnetization curls in plane around a core, where it points up or down *out of plane*.

Figure 1(b) shows the longitudinal magnetoresistance $R_{XX}=V_{XX}/I_X$ at $T=0.89T_c$, with J parallel to the in-plane applied H.[11] The magnetoresistance is strongly hysteretic. When the field is swept from positive to negative magnetic saturation (or *vice versa,* solid/hollow circles), R_{XX} remains close to normal-state values and shows minima around the coercive fields. However, after demagnetization (black lines), a decrease in several orders of magnitude in resistance around $H=0$ characterizes the transition into the S state. Thus, the system can be either S or N around $H=0$, depending on the magnetic history. This bistability is controlled by

TABLE I. Samples parameters; Al film thickness t_{Al}, dot diameters $\varnothing$ and interdot distances d, critical temperatures T_c, N-state resistance R_N, sign P of the transverse resistance ($\pm$ appears when both are observed), and ratio between the maximum transverse and the N-state resistances $R_\perp^{max}/R_N$.

No.	t_{Al} (nm)	$\varnothing, d$ (nm)	T_c (K)	R_N (Ω)	P	$\dfrac{R_\perp^{max}}{R_N}$
P2	20	75, 120	1.37	3.10	$\pm$	0.05
P3	20	140, 180	1.39	3.17	$\pm$	0.14
P5	40	75, 120	1.42	1.58	$\pm$	0.07
P6	40	140, 180	1.42	1.69	$\pm$	0.05
V7	20	70, 120	1.25	6.60	$\pm$	0.06
V10	20	75, 115	1.28	9.57	$-$	0.07
V13	15	70, 120	1.37	4.37	$\pm$	0.06

a)Electronic mail: javier.villegas@thalesgroup.com.
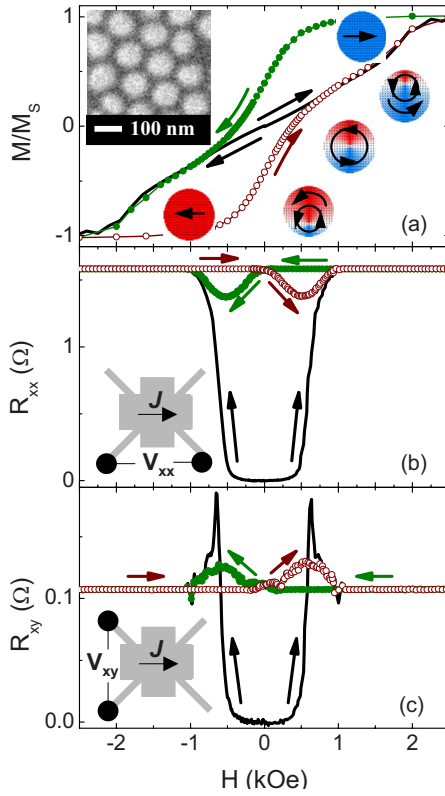b)Electronic mail: ischuller@ucsd.edu.

FIG. 1. (Color online) For sample P5: (a) in-plane magnetization (normalized to the magnetic saturation M_S) at $T=6$ K. Circles are for the major loop and the black lines for the virgin curves. Upper-left: typical scanning electron microscopy of the nanodot arrays. Lower-right: cartoon of the magnetic reversal mechanism. (b) Measured longitudinal and (c) transverse resistances vs applied magnetic field at $T=0.89T_c$ and $J=31.25$ kA cm^{-2}. Same symbols/line code as in (a). Insets in [(b) and (c)]: sketch of the electrical contact configurations.
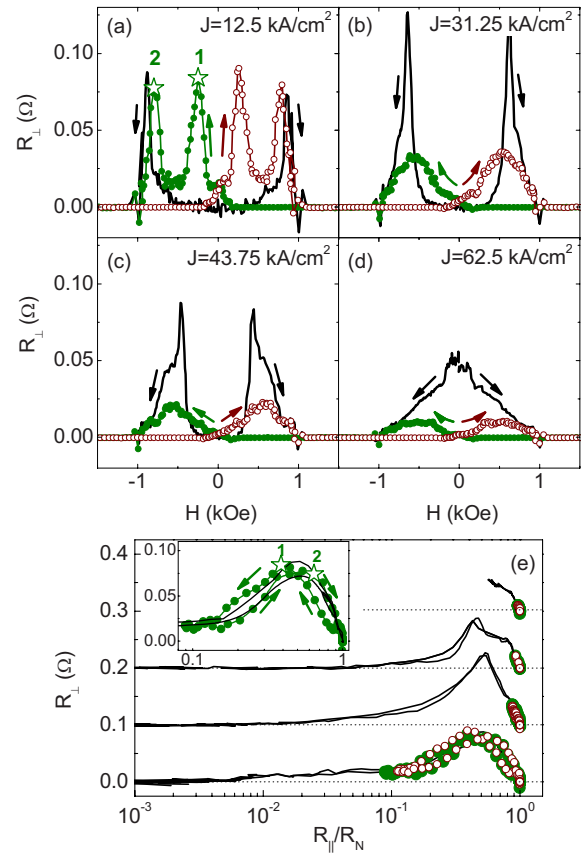

FIG. 2. (Color online) For sample P5: [(a)–(d)] pure transverse resistance as a function of the applied field at $T=0.89T_c$ for different current levels J. Solid (hollow) circles are for the major loop (measured from positive/negative saturation), black lines for the virgin curves. (e) Pure transverse resistance as a function of normalized longitudinal resistance $R_{\parallel}/R_N$ (R_N normal-state resistance). Same data and symbols/line code as in [(a)–(d)]. Curves for different $J=12.5$, 31.25, 43.75, and 62.5 kA cm^{-2} are shifted from bottom to top in steps of 0.1 Ω. Inset: zoom of the curve for $J=12.5$ kA cm^{-2}. The arrows show the sense of circulation for the curve measured from $R_{\parallel}/R_N=1$. The stars labeled 1 and 2 identify the corresponding data points in (a).

the stray magnetic fields from the nanodots (see Ref. 8), which induce a spatial modulation of the S condensate in the Al film. Within this picture, superconductivity is inhomogeneous: S and N domains coexist and the zero-resistance state develops as the S channels coalesce allowing the percolation of supercurrents.[8]

Figure 1(c) shows the transverse magnetoresistance $R_{XY}=V_{XY}/I_X$ at $T=0.89T_c$, with J parallel to the in-plane applied H.[11] R_{XY} is hysteretic and shows a very unusual behavior. When the field is swept from magnetic saturation (solid/hollow circles), R_{XY} peaks around the coercive field, reaching *above* the N-state value. After demagnetization (black lines), R_{XY} is much lower that in the N-state around $H=0$, then increases continuously as H is increased, and finally peaks reaching above the N-state value before saturation.

Due to minor misalignments of the voltage electrodes, the x (y) direction is not perfectly parallel (perpendicular) to the current J. Thus, the *measured* transverse resistance R_{XY} [Fig. 1(c)] contains some longitudinal component (and vice versa): i.e., $R_{XY}=R_{\perp}+\alpha R_{\parallel}$ and $R_{XX}=R_{\parallel}+\beta R_{\perp}$, where $R_{\perp}$ and $R_{\parallel}$ are the *pure* transverse and longitudinal resistances, and the coefficients α, β account for the electrodes misalignment. We obtained $\alpha \approx \beta \sim 0.1-0.15$ for all the samples from normal-state measurements, assuming that in this state $R_{\perp}=0$ and therefore $R_{XY}=\alpha R_{XX}$ and $R_{YX}=\beta R_{YY}$. This way we calculated *the pure transverse resistance* at any field/temperature $R_{\perp}=(R_{XY}-\alpha R_{XX})(1-\alpha\beta)^{-1}$.

Figures 2(a)–2(d) show $R_{\perp}(H)$ at $T=0.89T_c$ for several current levels J. $R_{\perp}$ exhibits a complicated current dependence. When the field is swept from positive (negative) saturation, the curves are asymmetric: a double peak [Fig. 2(a)] or a single broader peak [Figs. 2(b)–2(d)] appear at negative (positive) fields. After demagnetization (black lines) the curves are symmetric: depending on J, either two peaks [Figs. 2(a)–2(c)] at field values symmetric around $H=0$ or a single peak [Fig. 2(d)] at $H=0$ can be observed. Note that $R_{\perp}$ it is not an odd function of the applied field or the magnetization, which rules out conventional Hall effects.

Figure 2(e) shows $R_{\perp}$ as a function of the normalized *longitudinal* resistance $R_{\parallel}/R_N$ (R_N is the normal-state longitudinal resistance). Figure 2(e) contains the very same data as in Figs. 2(a)–2(d) (for clarity, data corresponding to different J are shifted vertically in steps of 0.1 Ω). The behavior of all samples is very similar, and has the following characteristics: (i) for each current J, $R_{\perp}$ versus $R_{\parallel}/R_N$, as field is swept from positive/negative magnetic saturation (solid/hollow circles) and after demagnetization (black lines) roughly collapse into a single master curve. $R_{\perp}$ is zero for $R_{\parallel}/R_N< \sim 10^{-3}$ (i.e., deep into the S state) and for $R_{\parallel}/R_N=1$ (i.e., in the N state), and increases from $R_{\parallel}/R_N \sim 10^{-1}$ to reach its maximum amplitude at around $R_{\parallel}/R_N \sim 0.4-0.8$; ii)
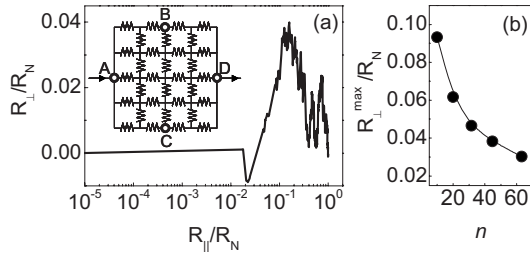
FIG. 3. (a) Computed transverse vs longitudinal resistance (both normalized to the *N*-state longitudinal resistance), for an array with $n=64$ ($n^2 \sim 4000$ resistors). The inset shows a sketch of the model for $n=4$ (voltage probes labeled A–D). (b) Maximum transverse resistance (normalized to the *N*-state longitudinal one) vs size n of the resistor array model.

a closer inspection [see inset in Fig. 2(e)] reveals fluctuations of up to 30% around the average $R_\perp$ versus $R_\parallel/R_N$, depending on the magnetic history (green circles) or upon repeated demagnetizations (dark lines); iii) while the overall behavior is similar for all current levels, as *J* is increased some of the curve details change, and the transition into the *S* state is gradually inhibited (i.e., the lower-limit of $R_\parallel/R_N$ increases); and iv) the maximum amplitude of the transverse signal $R_\perp^{max}$ scales with the normal-state longitudinal resistance R_N (the ratio $R_\perp^{max}/R_N \sim 0.05-0.07$ for most of the samples, see Table I). Besides the changes in the shape of $R_\perp$ versus $R_\parallel/R_N$, the sign of $R_\perp$ changes from sample to sample (and sometimes for a single sample depending on the injected current direction *x* or *y*), or even reverses as a function of $R_\parallel/R_N$. The sign(s) observed for each sample are listed on Table I. Note that measurements at different temperatures ($0.89T_C < T < 0.99T_C$) for different samples show no temperature effect on the magnitude of $R_\perp$. The only clear difference is that for higher temperatures the critical fields and currents are lower, which increases the lower-limit of $R_\parallel/R_N$.

We discuss below the origin of the anomalous transverse resistance $R_\perp$. Several flux-dynamics related mechanisms, such as the interaction between flux quanta with opposite polarities[4] or guided flux motion,[12] may result in even Hall effects in the *S* state. We ruled these out because here $R_\perp$ is independent of (i) the magnitude of the applied field (or density of flux quanta), and (ii) the Lorentz force.[11] Other mechanisms for resistance anomalies in *S* systems, such as charge imbalance effects[5,6] or *S* fluctuations induced by granularity,[13] are unlikely here because they always imply a large "excess" resistance (comparable to R_N) in the longitudinal direction, which we did not observe. We show below that the origin of the transverse resistance resides in current redistributions due to inhomogeneous superconductivity. The typical intrinsic inhomogeneity of evaporated Al films[5] is enhanced here because the stray field profile from the nanodots induces a spatial modulation of T_C.[8] If *N* and *S* regions coexist at a given *T*, the injected current will flow along the lowest resistance path, meandering across *N* regions that connect *S* ones. Thus, the current distribution will change across the phase transition as *N* regions gradually become *S* (or vice versa), and in this situation voltage probes which are not collinear with the overall current flow direction will measure a varying "excess"[14] or "negative" resistance.[15] We developed a simple model to check if these effects can account for the experimental $R_\perp$ versus $R_\parallel/R_N$ curves shown in Fig. 2(e). We used an array with $n \times n$ resistors, each of them having equal *N*-state resistance [see the inset of Fig. 3(a) for

a sketch; the current I_{AD} flows from A to D]. To simulate the inhomogeneous *N*-to-*S* transition, we randomly switched the resistors from their *N*-state value to zero, one at a time. We calculated the longitudinal and transverse array resistances at each step as $R_\parallel=V_{AD}/I_{AD}$ and $R_\perp=V_{BC}/I_{AD}$, respectively. Figure 3(a) shows an example of the $R_\perp/R_N$ versus $R_\parallel/R_N$ calculations, which are in good qualitative and quantitative agreement with the experimental curves. Moreover, the randomness in the sign (see Table I) and the fluctuations in the shape of $R_\perp$ versus $R_\parallel/R_N$ observed experimentally are mimicked by simulations upon repetitive realizations for a given array. Fluctuations induced in the experiments by (i) the magnetic history and ii) changes in the current level *J* are explained by the different spatial distribution of *S*/*N* domains (and thus different current meander paths) expected for (i) different magnetic states of the array[8] and (ii) produced as *J* locally overcomes the critical current of certain *S* domains. This model does not explicitly consider correlations between resistors. However, we can use the transverse resistance dependence on the size *n* of the array to estimate the correlations in real samples, by assuming that larger arrays imply smaller *N*/*S* domains (i.e., shorter correlations), and vice versa. Figure 3(b) shows the maximum amplitude of the transverse resistance $R_\perp^{max}/R_N$ versus the size *n* of the array.[16] The calculated $R_\perp^{max}/R_N$ values are comparable to the experimental ones for $n \sim 10-60$; in particular, the typical experimental $R_\perp^{max}/R_N \sim 0.06$ (see Table I) is obtained for $n \sim 20$. From this, and considering the width of the measuring bridge $w=40$ μm, we estimate that the characteristic length scale of the *N*/*S* domains is about $w/n \sim 2$ μm.

In conclusion, we have studied a hybrid *S*/*F* system which shows an anomalous, strongly hysteretic transverse magnetoresistance with a complicated current dependence. These effects are produced by current redistributions due to inhomogeneous superconductivity across the *S*-to-*N* phase transition.

[1] A. I. Buzdin, Rev. Mod. Phys. **77**, 935 (2005).
[2] I. F. Lyuksyutov and V. L. Pokrovsky, Adv. Phys. **54**, 67 (2005).
[3] R. Held, J. Xu, A. Schmehl, C. W. Schneider, J. Mannhart, and M. R. Beasley, Appl. Phys. Lett. **89**, 163509 (2006).
[4] L. I. Glazman, Sov. J. Low Temp. Phys. **12**, 389 (1986).
[5] P. Santhanam, C. C. Chi, S. J. Wind, M. J. Brady, and J. J. Bucchignano, Phys. Rev. Lett. **66**, 2254 (1991).
[6] M. Park, M. S. Isaacson, and J. M. Parpia, Phys. Rev. Lett. **75**, 3740 (1995).
[7] C.-P. Li, I. V. Roshchin, X. Batlle, M. Viret, F. Ott, and I. K. Schuller, J. Appl. Phys. **100**, 074318 (2006).
[8] J. E. Villegas, C.-P. Li, and I. K. Schuller, Phys. Rev. Lett. **99**, 227001 (2007).
[9] R. K. Dumas, C.-P. Li, I. V. Roshchin, I. K. Schuller, and K. Liu, Phys. Rev. B **75**, 134405 (2007).
[10] H. F. Ding, A. K. Schmid, D. Li, K. Yu. Guslienko, and S. D. Bader, Phys. Rev. Lett. **94**, 157202 (2005).
[11] We observed similar results with *J* perpendicular or parallel to *H*.
[12] J. E. Villegas, E. M. González, M. I. Montero, I. K. Schuller, and J. L. Vicent, Phys. Rev. B **68**, 224504 (2003); **72**, 064507 (2005).
[13] J. Hua, Z. L. Xiao, D. Rosenmann, I. Beloborodov, U. Welp, W. K. Kwok, and G. W. Crabtree, Appl. Phys. Lett. **90**, 072507 (2007).
[14] R. Vaglio, C. Attanasio, L. Maritato, and A. Ruosi, Phys. Rev. B **47**, 15302 (1993).
[15] J. Jorritsma and J. A. Mydosh, Phys. Rev. B **62**, 9703 (2000).
[16] We averaged $R_\perp^{max}/R_N$ over ten realizations for each *n*.